Polyhedron 31 (2012) 697–703

Contents lists available at SciVerse ScienceDirect

Polyhedron

journal homepage: www.elsevier.com/locate/poly

Structural properties and antibacterial potency of new supramolecular organotin(IV) dithiocarboxylates

Farzana Shaheen [a], Zia-ur-Rehman [a,*], Saqib Ali [a,*], Auke Meetsma [b]

[a] Department of Chemistry, Quaid-i-Azam University, Islamabad 45320, Pakistan
[b] Crystal Structure Center, Chemical Physics, Zernike, Institute for Advanced Materials, University of Groningen, Nijenborgh 4, NL-9747 AG Groningen, The Netherlands

ARTICLE INFO

Article history:
Received 29 September 2011
Accepted 24 October 2011
Available online 4 November 2011

Keywords:
Organotin(IV)
Dithiocarboxylate
NMR
X-ray
Antibacterial

ABSTRACT

A series of new organotin(IV) derivatives; Me_3SnL (**1**), Bu_3SnL (**2**), Ph_3SnL (**3**), Me_2SnClL (**4**), Bu_2SnClL (**5**), Ph_2SnClL (**6**), Et_2SnClL (**7**) and Et_2SnL_2 (**8**) where L = *N*-(2,3-dimethylphenyl)piperazine-1-carbodithioate have been synthesized and characterized by various analytical techniques. Among these techniques, ^1H and ^{13}C NMR were carried out to asses solution structures whereas the solid state structures were confirmed by FT-IR and X-ray single crystal analysis (**3**, **5** and **8**). Crystal structure of complex (**3**) and (**5**) showed distorted trigonal bipyramidal geometry and square pyramidal geometry, respectively. The inclination of the structure **5** towards square-pyramidal may be due to the presence of the Sn–Cl···HN-piperazine hydrogen bonds between the adjacent molecules. A supramolecular structure is shown by compound (**8**), with central tin atom exists in a distorted octahedral geometry. The antibacterial results indicated the profound activity of the compounds against various strains of bacteria. In addition to this, the triorganotin(IV) derivatives were found more active than diorganotin(IV) compounds.

1. Introduction

The coordination chemistry of sulfur-donor ligands is an area of focusing due to their close resemblance with biomolecules like amino acids (e.g. methionine, cysteine), peptides such as glutathione, proteins, enzymes and vitamins [1]. Among the various organosulfur systems, dithiocarboxylates and their metal complexes owe special significance due to their use as catalysts, in the rubber industry and in pesticides [2]. Antitumor and antiviral activities have been reported for pyrrolidine dithiocarboxylates salts [3]. Diethyldithiocarboxylate salts have been investigated for possible application in chronic alcoholic therapy [4] and treatment of HIV-patients [5]. Organotin(IV) dithiocarboxylates continue to attract significant attention because of their broad spectrum of biological applications as fungicides, bactericides, insecticides and antitumor agents [6]. Although number of efforts has been made to explore the mechanism of the biological action of organotin derivatives yet none of them is up to the mark. One group believed that the release of K^+ from cells, resulting from increased cytoplasmic membrane permeability, shows the cytoplasmic membrane to be a possible site of action [7]. The crossing of the cytoplasmic membrane by organotin derivatives might be a consequence of lipid-solubility [8] affected by weak interactions with the amino acids, proteins, nucleosides, carbohydrates and steroids present in the cell membrane [9,10]. Another proposition relates to the redox potential (0.154 V) for the conversion of Sn(IV) to Sn(II) that lies within the physiological range found for several enzyme reactions, thus suggesting that enzymatic processes might be involved in the biological activity of organotin compounds [11]. Our group recently reported with experimental evidences that biological action of the organotin is owing to their intercalative and electrostatic interaction with DNA [12,13]. In order to fortify this idea and keeping in view the antimicrobial potential of organotins, we synthesized eight organotin(IV) *N*-(2,3-dimethylphenyl)piperazine-1-carbodithioates having the capability of forming secondary interactions with cell constituents (see packing diagrams). These compounds proved to be effective antibacterial agents. This study will be helpful in designing new organotins of pharmaceutical value.

2. Experimental

2.1. Materials and methods

All the chemicals used in synthetic work were of high purity. Analytical grade organotin(IV) chlorides were purchased from Aldrich and Fluka chemical company. CS_2 was obtained from Reidel-de-Haën. Various solvents such as chloroform, methanol, toluene, *n*-hexane, ethanol, acetone and DMSO of analytical grade

* Corresponding authors. Tel.: +92 051 90642245; fax: +92 051 90642241 (Zia-ur-Rehman), tel.: +92 051 90642130; fax: +92 051 90642241 (S. Ali).
E-mail addresses: hafizqau@yahoo.com (Zia-ur-Rehman), drsa54@yahoo.com (S. Ali).

0277-5387/$ - see front matter © 2011 Elsevier Ltd. All rights reserved.
doi:10.1016/j.poly.2011.10.025

were purchased from E-Merk and Fluka. Solvents were dried by standard procedures [14].

Melting points were determined in capillary tube using electrothermal melting point apparatus model MP-D Mitamura Riken Kogyo (Japan) and are uncorrected. Elemental analysis was done using a Leco CHNS 932 apparatus. Infrared spectra were recorded as KBr disks on Perkin Elmer spectrum 1000 (USA) in range of 4000–250 cm^{-1}. ^1H NMR and ^{13}C NMR were recorded on Bruker AC 300 MHFT-NMR in chloroform.

The X-ray diffraction data were collected on a Bruker SMART APEX CCD diffractometer, equipped with a 4 K CCD detector. Data integration and global cell refinement was performed with the program SAINT. The program suite SAINTPLUS was used for space group determination (XPREP). The structure was solved by Patterson method; extension of the model was accomplished by direct method and applied to different structure factors using the program DIRDIF. All refinement calculations and graphics were performed with the program PLUTO and PLATON package [15]. The hydrogen atoms were generated by geometrical considerations, constrained to idealized geometries, and allowed to ride on the carrier atoms with an isotropic displacement parameter related to the equivalent displacement parameter of their carrier atoms, with U_{iso}(-H) = 1.2U_{eq}(C) or 1.5U_{eq}(methyl C). The methyl-groups were refined as rigid groups, which were allowed to rotate freely. Assigned values of bond distances: secondary C–H_2 = 0.99 Å, methyl C–H_3 = 0.98 Å and aromatic C–H = 0.95 Å.

2.2. Synthesis

2.2.1. Synthesis of N-(2,3-dimethylphenyl)piperazinium N-(2,3-dimethylphenyl) piperazine-1-carbodithioic acid (L-salt)

Insertion method was utilized for the synthesis of ligand. About 1.32 mL (0.02 mol) of CS_2 was added drop wise to a solution of *N*-(2,3-dimethylphenyl)piperazine (0.04 mol) in dry methanol. The reaction mixture was stirred for 4 h. Temperature was maintained at 273 K to avoid any possible decomposition. The white precipitates obtained were filtered and washed with diethyl ether. Yield: 7.8 g, 82%. M.p. 182–185 °C. *Anal.* Calc. for $C_{25}H_{36}N_4S_2$: C, 65.75; H, 7.95; N, 12.27; S, 14.04. Found: C, 65.05; H, 8.16; N, 12.23; S, 13.92%. FT-IR (cm^{-1}): 1014 ν(C–S), 1458 ν(C–N). ^1H NMR (ppm): 2.30 (s, $H_{11,11a}$), 2.24 (s, $H_{10,10a}$), 7.28–7.12 (m, $H_{7,7a,\ 6,6a,\ 5,5a}$), 4.69–4.63, 3.22–3.19 (m, $H_{3,3,\ 3a,\ 3a}$), 2.97–2.94, 2.31–2.24 (m, $H_{2,2,\ 2a,\ 2a}$), 8.46 (s, NH). ^{13}C NMR (ppm): 213.6 (C-1), 49.9, 45.0 (C-2,2′), 52.4, 51.2 (C-3,3′, 3a, 3′a), 151.6, 150.8, 138.0, 137.7, 131.1, 131.0, 126.3, 126.2, 125.8, 125.2, 117.3, 117.0 (Ar-C), 14.1 (C-10,10a), 20.7 (C-11,11a).

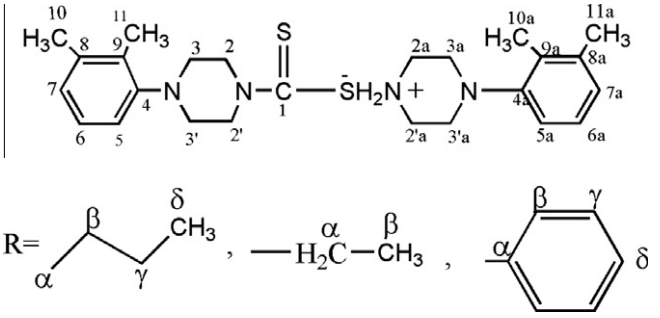

Scheme 1. Numbering scheme of ligand-salt and organic groups.

2.2.2. General procedure for synthesis of complexes

Triorganotin chloride or diorganotin dichloride and ligand salt were added to dry toluene in appropriate molar ratio. The mixture was allowed to reflux for 6–7 h with constant stirring. Soluble product was isolated by filtration and the solvent was rotary evaporated to get the desired product, which was then recrystallized from methanol chloroform mixture (Scheme 2). The numbering scheme of ligand-salt and organic groups is given in Scheme 1.

2.2.3. Synthesis of trimethylstannyl N-(2,3-dimethylphenyl)piperazine-1-carbodithioate (*1*)

Yield: 0.51 g, 68%. M.p. 111–113 °C. *Anal.* Calc. for $C_{16}H_{26}N_2S_2Sn$: C, 44.77; H, 6.11; N, 6.53; S, 14.94. Found: C,

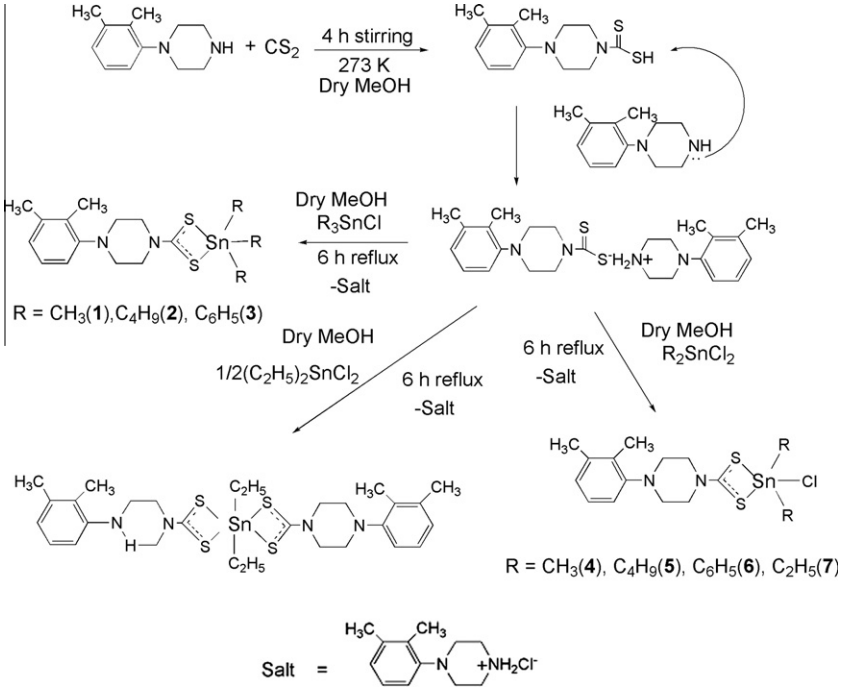

Scheme 2. Synthesis of ligand-salt and their organotin(IV) compounds.

45.71; H, 6.48; N, 6.47; S, 14.06%. FT-IR (cm^{-1}): 995 $\nu(CS_2)_{sym}$, 1108 $\nu(CS_2)_{asym}$, 1460 ν(C–N), 368 ν(Sn–S), 468 ν(Sn–C), ^{1}H NMR (ppm), $^2J[^{119}Sn–^1H, Hz]$: 2.31 (s, H_{11}), 2.26 (s, H_{10}), 6.86–7.11 (m, $H_{7,\ 6,\ 5}$), 3.09–3.12 (m, $H'_{3,3}$), 2.96–2.99 (m, $H'_{2,2}$), 0.66 [57, $\theta = 111°$] (s, H_3C–Sn) ^{13}C NMR (ppm): 198.3. (C-1), 116.9, 117.0, 125.7, 126.0, 131.4, 138.2, 150.4 (C–Ar), 52.1 (C-2, 2′), 51.6 (C-3, 3′), 0.8 {(H_3C–Sn), $^1J[^{119}Sn–^{13}C = 383, \theta = 110°]$}.

2.2.4. Synthesis of tributylstannyl N-(2,3-dimethylphenyl)piperazine-1-carbodithioate (2)

Yield: 0.64 g, 66%. M.p. 52–54 °C. *Anal.* Calc. for $C_{25}H_{44}N_2S_2Sn$: C, 54.06; H, 7.98; N, 5.04; S, 11.55. Found: C, 54.68; H, 7.98; N, 5.16; S, 11.89%. FT-IR (cm^{-1}): 975 $\nu(CS_2)_{asym}$, 1117 $\nu(CS_2)_{asym}$, 1465 ν(C–N), 354 ν(Sn–S), 468 ν(Sn–C). ^{1}H NMR (ppm): 2.19 (s, H_{11}), 2.15 (s, H_{10}), 6.89–7.14 (m, $H_{7,\ 6,\ 5,}$), 2.96–2.99 (m, $H'_{3,3}$), 2.27–2.30 (m, $H'_{2,2}$), 1.33–1.72 (m, $H_{\alpha,\beta,\gamma,\delta}$). ^{13}C NMR (ppm): 198.9 (C-1), 116.8, 125.7, 125.9, 131.4, 138.2, 150.5 (C–Ar), 52.1 (C-2,2′), 51.7 (C-3,3′), 28.9 {(C-α), $^1J[^{119}Sn–^{13}C = 349$ Hz, $\theta = 107°]$}, 27.1 (C-β), 17.8 (C-γ), 20.12 (C-δ).

2.2.5. Synthesis of triphenylstannyl N-(2,3-dimethylphenyl)piperazine-1-carbodithioate (3)

Yield: 0.68 g, 62.9%. M.p. 170–172 °C. *Anal.* Calc. for $C_{31}H_{32}N_2S_2Sn$: C, 60.50; H, 5.24; N, 4.55; S, 10.42. Found: C, 59.97; H, 5.3; N, 4.58; S, 10.19%. FT-IR (cm^{-1}): 977 $\nu(CS_2)_{sym}$, 1120 $\nu(CS_2)_{asym}$, 1460 ν(C–N), 351 ν(Sn–S). ^{1}H NMR (ppm): 2.30 (s, H_{11}), 2.25 (s, H_{10}), 6.89–7.14 (m, $H_{7,\ 6,\ 5,}$), 3.14–3.11 (m, $H'_{3,3}$), 2.96–2.99 (m, $H'_{2,2}$) 7.38–7.88 (m, $H_{\alpha,\beta,\gamma,\delta}$). ^{13}C NMR (ppm): 196.4 (C-1), 116.9, 125.1, 125.9, 131.4, 138.3, 151.8 (C–Ar), 52.8 (C-2, 2′), 51.6 (C-3, 3′), 142.2 {(C-α), $^1J[^{119}Sn–^{13}C = 605$ Hz]}, 128.6 (C-β), 136.7 (C-γ), 129.2 (C-δ).

2.2.6. Synthesis of chlorodimethylstannyl N-(2,3-dimethylphenyl)piperazine-1-carbodithioate (4)

Yield: 0.49 g, 62.8%. M.p. 169–170 °C. *Anal.* Calc. for $C_{15}H_{23}N_2S_2SnCl$: C, 40.07; H, 5.16; N, 6.23; S, 14.26. Found: C, 39.8; H, 5.02; N, 6.12; S, 13.87%. FT-IR (cm^{-1}): 987 $\nu(CS_2)_{sym}$, 1116 $\nu(CS_2)_{asym}$, 1462 ν(C–N), 364 ν(Sn–S), 493 ν(Sn–C), 267 ν(Sn–Cl), ^{1}H NMR (ppm) {$^2J[^{119}Sn–^1H, Hz]$}: 2.25 (s, H_{11}), 2.21 (s, H_{10}) [81, $\theta = 126°$], 6.90–7.15 (m, $H_{7,\ 6,\ 5,}$), 3.01–3.05 (m, $H'_{3,3}$), 2.26–2.31 (m, $H'_{2,2}$), 1.58 (H_3C–Sn) ^{13}C NMR (ppm): 196.7 (C-1), 116.9, 126.1, 126.2, 131.4, 138.4, 149.8 (C–Ar), 52.2 (C-2, 2′), 51.4 (C-3, 3′), 22.7 {(C–Sn), $^1J[^{119}Sn–^{13}C = 563$ Hz, $\theta = 126°]$}.

2.2.7. Synthesis of chlorodibutylstannyl N-(2,3-dimethylphenyl)piperazine-1-carbodithioate (5)

Yield: 0.61 g, 65.5%. M.p. 98 °C. *Anal.* Calc. for $C_{21}H_{35}N_2S_2SnCl$: C, 47.25; H, 6.61; N, 5.25; S, 12.01. Found: C, 47. 91; H, 6.44; N, 4.99; S, 11.12%. FT-IR (cm^{-1}): 997 $\nu(CS_2)_{sym}$, 1115 $\nu(CS_2)_{asym}$, 1473 ν(C–N), 372 ν(Sn–S), 418 ν(Sn–C), 261 ν(Sn–Cl), ^{1}H NMR (ppm): 2.19 (s, H_{11}), 2.15 (s, H_{12}), 6.89–7.14 (m, $H_{7,\ 6,\ 5,}$), 3.01–3.04 (m, $H'_{3,3}$), 2.27–2.30 (m, $H'_{2,2}$) 0.96–1.91 (m, $H_{\alpha,\beta,\gamma,\delta}$). ^{13}C NMR (ppm): 197.3 (C-1), 154.0, 149.8, 138.4, 131.4, 126.1, 116.9 (C–Ar), 52.2 (C-2, 2′), 51.4 (C-3, 3′), 26.3 (C-α), 27.8 (C-β), 29.2 (C-γ), 29.7 (C-δ).

2.2.8. Synthesis of chlorodiphenylstannyl N-(2,3-dimethylphenyl)piperazine-1-carbodithioate (6)

Yield: 0.68 g, 67.5%. M.p. 147–149 °C. *Anal.* Calc. for $C_{25}H_{27}N_2S_2SnCl$: C, 52.33; H, 4.74; N, 4.88; S, 11.18. Found: C, 51.88; H, 4.93; N, 4.92; S, 10.95%. FT-IR (cm^{-1}): 992 $\nu(CS_2)_{sym}$, 1120 $\nu(CS_2)_{asym}$, 1463 ν(C–N), 372 ν(Sn–S), 263 ν(Sn–Cl). ^{1}H NMR (ppm): 2.34 (s, H_{11}), 2.30 (s, H_{12}), 6.89–7.15 (m, $H_{7,\ 6,\ 5,}$), 2.27–2.32 (m, $H'_{3,3}$), 3.02–3.05 (m, $H'_{2,2}$) 7.46–8.13 (m, $H_{\alpha,\beta,\gamma,\delta}$). ^{13}C NMR (ppm): 195.9 (C-1), 117.0, 126.1, 126.2, 128.3, 136.2, 149.7 (C–Ar), 52.9 (C-2, 2′), 51.3 (C-3, 3′), 128.8 (C-α) 135.7 (C-β), 130.3 (C-γ), 138.4 (C-δ).

2.2.9. Synthesis of chlorodiethylylstannyl N-(2,3-dimethylphenyl)piperazine-1-carbodithioate (7)

Yield: 0.56 g, 66.6%. M.p. 103–104 °C. *Anal.* Calc. for $C_{17}H_{27}N_2S_2SnCl$: C, 42.74; H, 5.70; N, 5.86; S, 13.42. Found: C, 42.75; H, 5.66; N, 5.94; S, 13.40%. FT-IR (cm^{-1}): 991 $\nu(CS_2)_{sym}$, 1114 $\nu(C–S)_{asym}$, 1460 ν(C–N), 360 ν(Sn–S), 473 ν(Sn–C), 265 ν(Sn–Cl). ^{1}H NMR (ppm) ^{1}H 2.31 (s, H_{11}), 2.26 (s, H_{12}), 6.90–7.15 (m, $H_{7,7a,\ 6,6a,\ 5,5a}$), 3.01–3.04 (m, $H'_{3,3}$), 2.26–2.31 (m, $H'_{2,2}$) 2.12 (q, H_α, $^3J_{H–H} = 16$Hz), 1.61 (t, H_β, $^3J_{H–H} = 16$Hz). ^{13}C NMR (ppm): 197.2 (C-1), 149.8, 138.4, 131.4, 126.1, 125.6, 116.9 (C–Ar), 52.2 (C-2, 2′), 51.4 (C-3, 3′), 21.3 {(C-α) $^1J[^{119}Sn–^{13}C = 533$ Hz, $\theta = 123.5°]$}, 10.3 (C-β).

2.2.10. Synthesis of diethylstannyl bis[N-(2,3-dimethylphenyl)piperazine-1-carbodithioate] (8)

Yield: 0.53 g, 67.9%. M.p. 220–222 °C. *Anal.* Calc. for $C_{30}H_{44}N_4S_4Sn$: C, 50.92; H, 6.27; N, 7.92; S, 18.12. Found: C, 50.49; H, 6.30; N, 7.60; S, 17.89%. FT-IR (cm^{-1}): 991 $\nu(CS_2)_{sym}$, 1113 $\nu(CS_2)_{sym,}$ 1460 ν(C–N), 356 ν(Sn–S), 480 ν(Sn–C), 261. ^{1}H NMR (ppm): 2.27 (s, H_{11}), 2.25 (s, H_{10}), 6.90–7.15 (m, $H_{7,\ 6,\ 5,}$), 3.01–2.97 (m, $H'_{3,3}$), 2.31–2.28 (m, $H'_{2,2}$). 2.12 (q, CH_2, $SnEt_2$, $^3J_{H–H} = 15$ Hz), 1.61 (t, CH_3, $SnEt_2$, $^3J_{H–H} = 15$ Hz). ^{13}C NMR (ppm): 200.8 (C-1), 51.6 (C-2, 2′), 50.6 (C-3, 3′, 3a, 3′a), 150.4, 138.2, 131.41, 126.0, 125.8, 116.9 (Ar–C), 13.9 (C-7), 20.7 (C-8), 29.7 {(C-α), $^1J[^{119}Sn–^{13}C = 545$ Hz, $\theta = 124.5°]$}, 10.9 (C-β).

2.2.11. Antibacterial evaluation

The synthesized compounds were tested for antibacterial activity against four different bacterial strains including, *Staphylococcus aureus* (G^+), *Bacillus subtilis* (G^+), *Pseudomonas aeruginosa* (G^-) and *Escherichia coli* (G^-) using the agar well diffusion method [16]. Ampicillin was used as standard drug and the wells (6 mm in diameter) were dug in the media with the help of a sterile metallic borer. Two to eight hours old bacterial inoculums containing approximately 10^4–10^6 colony forming units (CFU)/mL were spread on the surface of a nutrient agar with the help of a sterile cotton swab. The recommended concentration of the test sample (2 mg/mL in DMSO) was introduced into the respective wells. Other wells supplemented with DMSO and reference antibacterial drug served as negative and positive controls, respectively. The plates were incubated immediately at 37 °C for 20 h. The activity was determined by measuring the diameter of the inhibition zone (in mm), showing complete inhibition. Growth inhibition was calculated with reference to the positive control.

3. Results and discussion

3.1. FT-IR spectral data

FT-IR band values related to different functional groups have been assigned by comparison of the FT-IR spectra of the complexes with their related precursors. New absorption bands appeared in the region 414–480 cm^{-1} and 351–372 cm^{-1} can be assigned to Sn–C and Sn–S stretching mode of vibrations, respectively. These values are in close agreement with that observed for a number of organotin(IV)–sulfur donor ligands [17].

The two bands related C–S and C–N stretching vibrations give valuable information about the coordination behavior of dithiocarboxylate ligand to Sn atom, and thus give a clue about structure of complexes. FT-IR spectra of complexes **1**–**3** gave strong peaks at 1120–1108 cm^{-1}, that can be attributed to the asymmetric absorption of $\nu(CS_2)_{as}$ and the 997–977 cm^{-1} can be assigned to the symmetric $\nu(CS_2)_s$ absorption frequencies. The difference of $\nu(CS_2)_{as}$ and $\nu(CS_2)_s$ are 113–135 cm^{-1}, that is an indication of bidentate binding of the ligand to the central tin atom [17]. The stretching

Table 1
Crystal refinement data for complexes (**3**), (**5**) and (**8**).

Moiety formula	$C_{31}H_{32}N_2S_2Sn$ (**3**)	$C_{21}H_{35}S_2N_2SnCl$ (**5**)	$(C_{15}H_{22}N_2S_2)_2Sn$ (**8**)
Formula weight (g mol^{-1})	615.45	533.81	707.68
Crystal system	monoclinic	triclinic	monoclinic
Space group, no. 15	$P2_1/c$, 14	$P\bar{1}$, 2	$C2/c$, 15
a (Å)	19.062(2)	10.0753(10)	28.212(2)
b (Å)	7.4576(9)	14.4811(15)	7.2985(6)
c (Å)	20.624(2)	18.4442(19)	17.0056(14)
α (°)		113.0520(10)	
β (°)	103.963(2)	94.9270(10)	113.2900(10)
γ (°)		94.4040(10)	
V (Å^3)	2845.2(5)	2449.1(4)	3216.2(4)
θ Range for data collections (°)	2.54–27.39	2.42–29.36	2.90–28.67
Z	4	4	4
Total reflections	15273	21949	14109
Independent reflections	6411	11600	3973
All			
For $F_o \geqslant 4.0\ \sigma\ (F_o)$	4769	9207	3462
$R(F) = \sum(\|\|F_o\| - \|F_c\|\|)/\sum\|F_o\|$	0.0356	0.0525	0.0308
For $F_o > 4.0\ \sigma\ (F_o)$			
$wR(F^2) = [\sum[w(F_o^2 - F_c^2)^2]/\sum[w(F_o^2)^2]]^{1/2}$	0.0863	0.1402	0.0749
Goodness-of-fit (GOF)	1.011	1.077	1.068
Color, habit	colorless, needle	colorless, cut-fragment	colorless, block
Crystal size (mm)	0.41 × 0.13 × 0.08	0.55 × 0.51 × 0.45	0.34 × 0.29 × 0.22

Table 2
Selected bond lengths(Å) and bond angles (°) for compound **3**.

Ph_3SnL (**3**)			
Sn–S1	3.0223(9)	Sn–C26	2.159(3)
Sn–S2	2.4740(8)	S1–C1	1.693(2)
Sn–C14	2.137(3)	S2–C1	1.754(3)
Sn–C20	2.146(3)		
S1–Sn–S2	64.40(2)	S2–Sn–C26	91.03(8)
S1–Sn–C14	86.26(8)	C14–Sn–C20	108.37(10)
S1–Sn–C20	88.84(8)	C14–Sn–C26	108.31(11)
S1–Sn–C26	155.27(8)	C20–Sn–C26	104.56(11)
S2–Sn–C14	115.60(8)	Sn–S1–C1	79.91(10)
S2–Sn–C20	125.43(7)	Sn–S2–C1	69.69(8)

vibration peaks of the C–N, were obtained at ~1458–1473 cm^{-1} and are intermediate between the values for C–N single bond (1250–1360 cm^{-1}) and C=N double bond (1640–1690 cm^{-1}). Partial double bond character for the C–N bond would result in some partial double bond character for the C–S bonds. The analyses are in agreement with X-ray single crystal diffraction results, obtained for complexes **3**, **5** and **8**.

3.2. NMR spectra

In case of all the complexes, the disappearance of duplicate peak pattern and appearance of new signals for organic group attached to Sn(IV) atom confirmed the formation of complexes **1**–**8**. The organic groups attached to Sn atom give signals in the expected regions. The coupling constant value obtained for **1** suggests tetrahedral geometry in solution. Similarly the angle value calculated from $^2J(^{119}Sn–^1H)$ coupling constant for complex **4** certify five coordinate environment around Sn [18].

In ^{13}C NMR of complexes **1**–**7**, the duplicate peak pattern due *N*-(2,3-dimethylphenyl)piperazinium ion disappeared upon complexation to Sn. In complexes ^{13}C chemical shift values observed were similar to that of the ligand except small shift in the position of C(1), which was due to deshielding of this carbon upon coordination of both the sulfur atoms with the Sn atom. The alkyl groups attached to Sn atom showed signals in the expected range. Coupling constant values obtained in case of **1**, **2**, **3**, **4**, **7** and **8** give information about the relevant geometry of complexes in solution. Possible geometry of **1**, evaluated by ^1H NMR was confirmed by ^{13}C NMR. Trimethyl-, tributyl- and triphenyltin complexes dissociated in solution and gave a tetrahedral geometry in solution state. Complex **8** dissociate in solution to give a five coordinate complex, whereas complex **7** retains its geometry in solution [19]. In compounds **5** and **6**, a complex peak pattern is observed which depicts no significant Sn satellites, and hence assignment of geometry is not possible. The angle values calculated for **1**, **2**, **4**, **7** and **8** verify geometry of these complexes in solution.

3.3. Crystal structure analysis

X-ray crystal structure provides most adequate information on the structure of crystalline compound. Upon dissolution in polar solvents, regular packing held together by coordination, electrostatic and H-bonds may be broken down. Therefore the results

Table 3
Selected bond lengths(Å) and bond angles (°) for two different molecules of compound **5**.

	$X = 1$	$X = 2$		$X = 1$	$X = 2$
Sn–Clx	2.4626(12)	2.4926(11)	Snx–Cx18	2.162(5)	2.116(5)
Snx–Sx1	2.4892(12)	2.4671(13)	Sx1–Cx1	1.743(4)	1.755(4)
Snx–Sx2	2.6986(12)	2.7416(11)	Sx2–Cx1	1.719(4)	1.709(5)
Snx–Cx14	2.129(6)	2.156(5)			
Clx–Snx–Sx1	85.58(4)	86.07(4)	Sx1–Snx–Cx18	116.90(16)	117.74(14)
Clx–Snx–Cx2	154.55(4)	154.90(4)	Sx2–Snx–Cx14	98.85(14)	94.26(11)
Clx–Snx–Cx14	95.95(14)	97.34(12)	Sx2–Snx–Cx18	87.80(11)	93.11(14)
Clx–Snx–Cx18	100.05(12)	95.65(14)	Snx–Sx1–Cx1	89.64(14)	90.65(15)
Sx1–Snx–Sx2	69.39(3)	69.06(4)	Snx–Sx2–Cx1	83.46(14)	82.80(14)
Sx1–Snx–Cx14	115.46(14)	109.52(13)	Cx14–Snx–Cx18	126.0(2)	131.62(19)

Table 4
Selected bond lengths(Å) and bond angles (°) for compound **8**.

Sn–S1	3.0304(7)	Sn–C14	2.140(2)
Sn–S2	2.5243(6)	Sn–C14a	2.140(2)
Sn–S1_a	3.0304(7)	S1–C1	1.689(2)
Sn–S2_a	2.5243(6)	S2–C1	1.755(2)
S1–Sn–S2	64.02(2)	S2–Sn–S1_a	143.13(2)
S1–Sn–C14	84.60(7)	S2–Sn–S2_a	79.33(2)
S1–Sn–S1_a	152.80(2)	S2–Sn–C14_a	105.37(6)
S1–Sn–S2_a	143.13(2)	C14–Sn–S1_a	84.77(7)
S1–Sn–C14_a	84.77(7)	C14–Sn–S2_a	105.37(6)
S2–Sn–C14	109.98(7)	C14–Sn–C14_a	133.57(9)

are not always applicable for the complexes existing in aqueous solutions, although many examples prove that the main binding sites are same in crystal and in solution [20].

Crystal refinement data for complexes (**3**), (**5**) and (**8**) are given in Table 1, and geometric parameters are listed in Table 2–4.

In complex (**3**) the geometry around tin can be best characterized by the τ value that can be calculated by using expression, $\tau = \beta - \alpha/60$. Here β and α, are two consecutive largest angles around Sn. τ value is 1 for perfect trigonal bipyramidal and zero for perfect square planar geometry. In case of this complex (**3**), the value of τ is 0.49 ascertaining the structure is a mid way between trigonal bipyramidal and square pyramidal [21]. At the axial positions of this distorted structure is C26 atom of phenyl group and S1 (Fig. 1) atom of ligand and define an angle value of 155.27(8)°. The presence of S1 at apical position is in accord with the Bent's rule that says the most electronegative atom should be at the axial position, on the basis of amount of s-character of the metal hybrid orbital used in bonding [22]. The presence of S1 at pseudo-axial position is due to chelation restrain of the four membered CS_2Sn ring. Consequently, the angle value with basal plane is reduced to 64.40(2)°. S2 from the ligand and two α-carbons of phenyl group construct an equatorial plan with S2–Sn–C14 = 115.60(8)°, S2–Sn–C20 = 125.43(7)°, C14–Sn–C20 = 108.37(10)°. The coordination of dithiocarboxylate ligand to the Sn center is anisobidentate as evident from unequal Sn–S bond lengths [Sn–S1 = 3.0223(9) Å and Sn–S2 = 2.4740(8) Å]. Similarly bond distance, C1–S1 = 1.693(2) Å, indicates strong binding of S1 than S2 [C1–S2 = 1.754(3) Å] with Sn center. The packing diagram illustrates the supramolecular structure for **3** mediated by S···H–Ar and NCH_2···H non-covalent intermolecular interactions (Fig. 2). The presence of S···H–Ar intermolecular interactions may be the second main cause of deviation of geometry from perfect trigonal-bipyramidal to square-pyramidal.

The asymmetric unit of complex **5** contains two different molecules. A molecular structure for one of the two independent

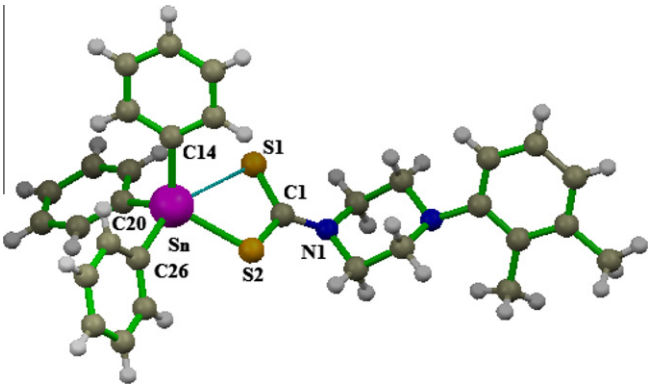

Fig. 1. Molecular structure of complex **3** with atomic numbering scheme.

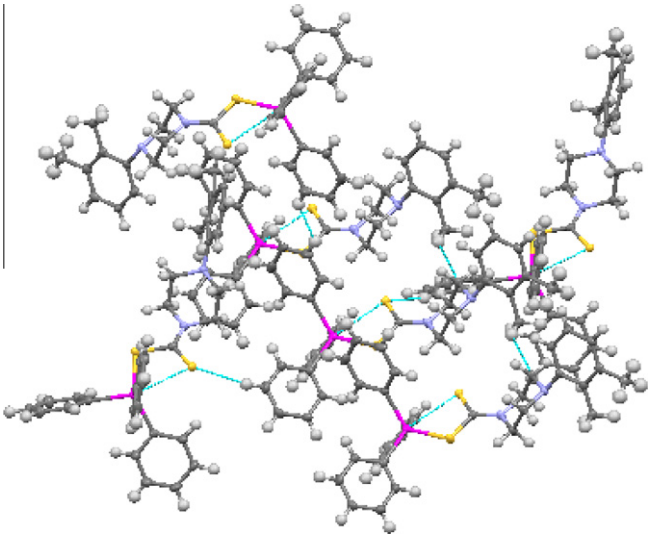

Fig. 2. Supramolecular structure of compound **3** mediated by S···H and H···CH_2N interactions.

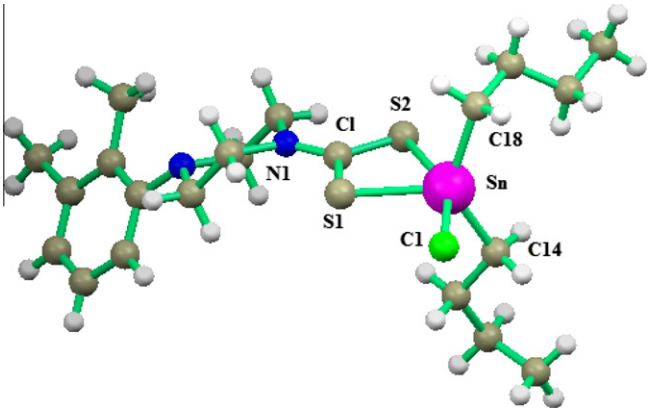

Fig. 3. Molecular structure of complex **5** with atomic numbering scheme.

molecules, together with an example of the partial atom numbering scheme used here is shown in Fig. 3. The configuration about the tin atom is five-coordinate. The sum of the equatorial angles involving the two α-carbons of the butyl groups and an S atom 358.36° and 358.88°, show little deviation from the ideal angle of 360°. The τ value for the two independent molecules is 0.47 and 0.38 that confirms highly distorted square-pyramidal geometry, especially for the later one (Table 3). The tendency of going from trigonal-bipyramidal geometry to square-pyramidal one may be due to the intermolecular SnCl···H_2CN interactions (Fig. 4). These interactions result in the supramolecular structure of the compound **5**. For each of the two independent molecules, the Cl atom occupies one of the apical positions of the highly distorted trigonal-bipyramid with the Cl1–Sn1–S12 and Cl2–Sn2–S22 angles of 154.55° and 154.90°, respectively. The quasi-axial S12 and S22 atoms cannot occupy exactly the position *trans* to Cl and Cl1–Sn1–S12 and Cl2–Sn2–S22 angles are 154.55(4)° and 154.90(4)°. Here again ring strain plays a significant role in an asymmetric bonding of the ligand, with shorter Sn1–S11 and Sn2–S21 bond lengths are [2.4892(12) and 2.4671(13) Å] and longer Sn1–S12 bond and Sn2–Sn22 [2.6986(12) and 2.7416(11) Å] respectively. The Sn–Cl bond length [2.4626(12)°] falls in the range of covalent radii of the two atoms (2.37–2.60 Å) [23].

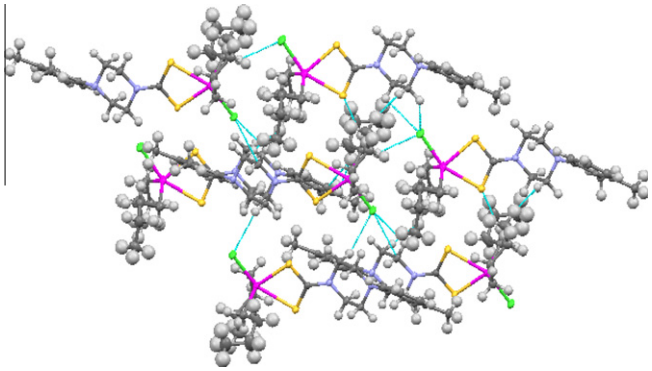

Fig. 4. Supramolecular structure of compound **5** mediated by Cl···H and Cl–H_2CN interactions.

Complex (**8**) shows a distorted octahedral geometry in which four S-atoms of the two chelating dithiocarboxylate ligands define the basal plane (Fig. 5). Ethyl groups occupy axial positions with C14–Sn–C14_a = 133.57(9)°. The value of $CSnC_{axial}$ shows that two ethyl groups do not occupy exact *trans* axial position thus results in distorted octahedral geometry. Likewise basal plane is also distorted from square planar geometry as cis S1–Sn–S1a angle is 152.80(2)° and cis S2–Sn–S2a is only 79.33(2)°. The two Sn–S bond lengths [Sn–S1 = 3.0304(7) and Sn–S2 = 2.5243(6) Å] are unequal, attesting the asymmetric coordination of ligand to Sn atom. In addition to this, Sn–S1 and Sn–S1a bond lengths are equivalent [3.0304(7) Å], same is the case with Sn–S2 and Sn–Sn2a bond lengths [2.5243(6) Å] confirming the same degree of asymmetry in the coordination of both ligands. Each shorter C–S bond is associated with longer Sn–S bond, further verified an asymmetric mode of coordination. The bond angles subtended at the tin atom by the methylene carbon with S2 and S2_a atoms are 109.98(7) and 105.37(6), respectively, which reveals that Sn–C bonds are bent towards longer Sn–S as a consequence of repulsion between bonding electron pairs around central Sn atom. Such structural deviations from the regular octahedral geometry can also be explicated on electronic and steric grounds. Thus, coordination geometry around Sn in compound **8** is best described as skew trapezoidal bipyramidal.

A comparison of Sn–S bond lengths among the compounds **3**, **5**, and **8** show that $Sn–S_{short}$ bond distances decreases in the order of **3** < **5** < **8** while $Sn–S_{long}$ bond distances decreases as **5** < **3** < **8**. The larger values of bond distances for **8** in both cases is due to two electron donating ethyl groups which decreases the electron accepting ability of central tin atom from the donor sulfur atoms, thus lengthening both the $Sn–S_{shorter}$ and $Sn–S_{longer}$ bond distances. As the two ethyl groups occupy *trans* axial positions, so impart similar effect for shorter and longer bond distances. Complex **3** shows smaller bond length value for $Sn–S_{short}$ than **5** but the trend is reverse in case of $Sn–S_{longer}$. This may be explained on the basis of planarity and electron withdrawing nature of the phenyl groups on Sn that make Sn electron greedy thus attracting the sulfur atom more closely to form shorter $Sn–S_{short}$ than **5**. The lengthening of $Sn–S_{longer}$ bond in **3** than **5** can be attributed to the involvement of this sulfur in S···H hydrogen bond (Fig. 2). Geometry of complexes imposes some additional effects on bond length values. Octahedral and trigonal bipyramidal geometry also contributes in defining behavior of Sn–S bond. In complex **8**, basal plan experiences more electronic repulsion (due to octahedral geometry) than trigonal plan (**3** and **5**), resulting in elongation of $Sn–S_{shorter}$ and $Sn–S_{longer}$ bonds.

A comparison of the τ values for the five-coordinate complexes **3** and **5** reveals the smallest value for complex **5**. The inclination of the later structure more towards square-pyramidal is because of the involvement of Sn–Cl moiety of one molecule in hydrogen bonding to the piperazine moiety of the molecule near by (Fig. 4).

3.4. Antibacterial activity

Free ligand and its organotin(IV) complexes were tested against four different strains of bacteria by agar well diffusion method.

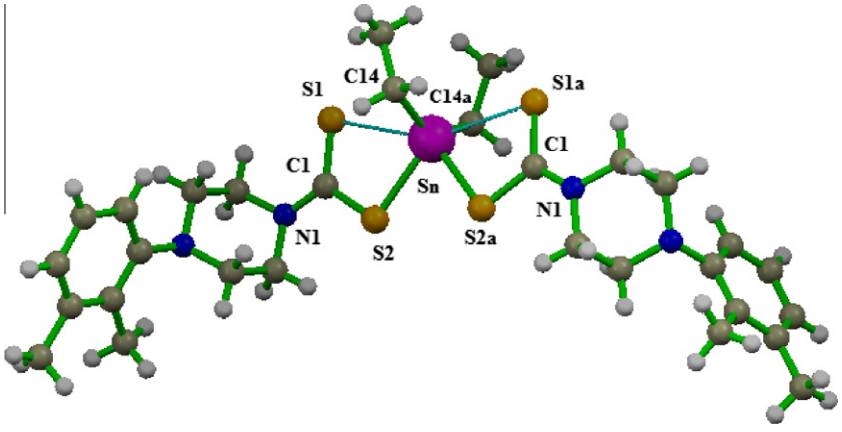

Fig. 5. Molecular structure of compound **8** with atomic numbering scheme.

Table 5
Antibacterial activity of organotin(IV) derivatives of S-donor ligand.

Name of bacteria	Zone of inhibition of sample (mm)									Standard drug[a]
	L	(**1**)	(**2**)	(**3**)	(**4**)	(**5**)	(**6**)	(**7**)	(**8**)	
Staphylococcus aureus	26	37	46	34	32	30	23		16	29
Bacillus subtilis	31	42	32	39	37	30	22		19	16
Pseudomonas aeruginosa	25	35	42	24	35	28	23		17	20
Escherichia coli	33	44	26	17	41	35	19		18	17

[a] Standard drug = ampicillin.

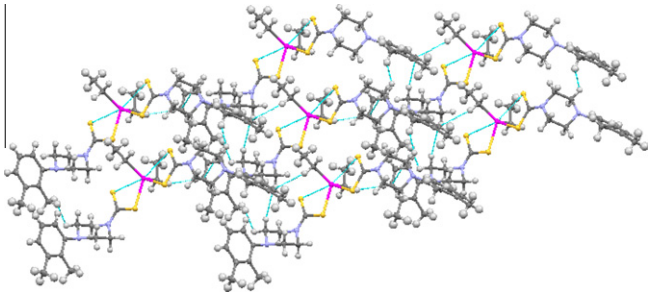

Fig. 6. Supramolecular structure of compound **8** mediated H···CH_2N interactions.

Antibacterial data is given in Table 5. The results obtained were quite promising, and in general complexes are more active than parent ligand. This shows that coordination with Sn(IV) atom is a good measure of improving activity of the ligand. The chelation reduces polarity of metal ion because of partial sharing of its positive charge with donor groups and possibly the delocalization by π-electron delocalization within whole chelate ring system that is formed during coordination. These factors increase the lipophilic nature of central metal atom, thus increasing the hydrophobic character and liposolubility of the molecule favouring its permeation through the lipid bilayers of bacterial membrane. This enhances the rate of uptake and thus antibacterial activity of testing compounds [24].

By comparing the activity with standard drug, it was found that in most cases complexes show more activity. In general, triorganotin(IV) complexes are found to be more active than diaorganotin(IV) complexes, a trend consistent with early reports [25].

The variation in trends for these compounds may be explained on the basis of three possible factors i.e. lipophilic character, diffusion and on the bacterial strain. The former two factors are associated with complexes. Lipophilic character decreases with increasing chain length whereas diffusion has an inverse effect. Enhanced activities of triorganotin complexes can be well described by the lipophilic character. In some of the cases diorganotin complexes were found more active e.g. in dimethyltin complexes due to dominating diffusive nature of small methyl group.

4. Conclusions

Eight new organotin(IV) derivatives of *N*-(2,3-dimethylphenyl)piperazine-1-carbodithioate have been synthesized and successfully characterized. Based on the X-ray single crystal analysis supramolecular structure can be attributed to compounds **3**, **5** and **8** in solid state. These compounds are valuable because of their promising antibacterial activities against various strains of bacteria. In addition to this, the triorganotin(IV) derivatives supersede the diorganotin(IV) compounds in their antibacterial action. Keeping in view the packing diagrams (Figs. 2, 4 and 6), it can be proposed that these compounds exert their antibacterial action by making similar kind of secondary non-covalent contacts with the cell constituents of microbes. Thus, hindering various cellular processes and ultimately causing death of the bacterium cell.

Acknowledgements

We thank the Higher Education Commission of Pakistan for financial support.

Appendix A. Supplementary data

CCDC 723568, 723569 and 723570 contain the supplementary crystallographic data for **8**, **5** and **3**. These data can be obtained free of charge via http://www.ccdc.cam.ac.uk/conts/retrieving.html, or from the Cambridge Crystallographic Data Centre, 12 Union Road, Cambridge CB2 1EZ, UK; fax: (+44) 1223-336-033; or e-mail: deposit@ccdc.cam.ac.uk.

References

[1] L.A. Komarnisky, R.J. Christopherson, Nutrition 19 (2003) 54.
[2] World Health Organization, Environ. Health Criter. 78 (1988) 1.
[3] (a) S.H. Kim, S.I. Han, S.Y. Oh, H.Y. Chung, H.D. Kim, H.S. Kang, Biochem. Biophys. Res. Commun. 281 (2001) 367;
(b) L. Malaguarnera, M.R. Pilastro, R. Di Marco, C. Scifo, M. Renis, M.C. Mazzarino, A. Messina, Apoptosis 8 (2003) 539;
(c) N. Uchide, K. Ohyama, J. Antimicrob. Chemother. 52 (2003) 8.
[4] C. Brewer, Alcohol Alchol 28 (1993) 383.
[5] J.M. Lang, J.L. Touraine, C. Trepo, P. Choutet, M. Kirstetter, A. Falkenrodt, L. Herviou, J.M. Livrozet, G. Retornaz, F. Touraine, Lancet 8613 (1988) 702.
[6] I. Baba, A.F.A. Muthalib, Y.F.A. Aziz, N.S. Weng, Phosphorus, Sulfur Silicon Relat. Elem. 186 (2011) 1326.
[7] J. S White, J.M. Tobin, J. Appl. Microbiol. Biotechnol. 63 (2004) 445.
[8] O.S. Laurence, J.J. Cooney, G.M. Gadd, Microb. Ecol. 17 (1989) 275.
[9] B.A. Buck-Koehntop, F. Porcelli, J.L. Lewin, C.J. Cramer, G.J. Veglia, Organomet. Chem. 691 (2006) 1748.
[10] D.C. Menezesa, F.T. Vieiraa, G.M. de Limaa, J.L. Wardellb, M.E. Cortesc, M.P. Ferreirad, M.A. Soarese, A.V. Boase, Appl. Organometal. Chem. 22 (2008) 221.
[11] J.M. Tsangaris, D.R. Williams, Appl. Organomet. Chem. 6 (1992) 3.
[12] Zia-ur-Rehman, A. Shah, N. Muhammad, S. Ali, R. Qureshi, I.S. Butler, J. Organomet. Chem. 694 (2009) 1998.
[13] Zia-ur-Rehman, A. Shah, N. Muhammad, S. Ali, R. Qureshi, I.S. Butler, Eur. J. Med. Chem. 44 (2009) 3986.
[14] W.F.L. Armarego, C. Chai, Purification of Laboratory Chemicals, fifth ed., Butterworth, Oxford, 2003.
[15] (a) A.L. Spek, PLATON, A Multipurpose Crystallographic Tool, Utrecht University, Utrecht, The Netherlands, 2008;
(b) A.L. Spek, J. Appl. Crystallogr. 36 (2003) 7.
[16] A. Rahman, M.I. Choudhary, W.J. Thomsen, Bioassay Techniques for Drug Development, Harwood Academic Publishers, The Netherlands, 2001. pp. 1–203.
[17] H.D. Yin, S.C. Xue, Appl. Organometal. Chem. 20 (2006) 283.
[18] T.P. Lockhart, W.F. Manders, E.M. Holt, J. Am. Chem. Soc. 108 (1986) 6611.
[19] T.S.B. Baul, S. Dhar, S.M. Pyke, E.R.T. Tiekink, E. Rivarola, R. Butcher, F.E. Smith, J. Organomet. Chem. 633 (2001) 7.
[20] B. Gyrucsik, L. Nagy, Coord. Chem. Rev. 203 (2000) 81.
[21] A.W. Addison, T.N. Rao, J. Reedijk, J. Van Rijn, G.C. Verschoor, J. Chem. Soc., Dalton Trans. (1984) 1349.
[22] J.E. Huheey, Inorg. Chem. 20 (1981) 4033.
[23] M. Hanif, M. Hussain, M. Bhatti, S. Ali, H.S. Evans, Struct. Chem. 19 (2008) 777.
[24] E.K. Efthimiadou, G. Psomas, Y. Sanakis, N. Katsarose, A. Karaliota, J. Inorg. Biochem. 101 (2007) 532.
[25] E.R.T. Tiekink, Appl. Organometal. Chem. 22 (2008) 533.